Quasiparticle energy spectra and magnetic response of certain curved graphitic geometries

L. Wang, P.S. Davids, A. Saxena, and A.R. Bishop

Theoretical Division and Centers for Nonlinear Studies and Materials Science, Los Alamos National Laboratory, Los Alamos, New Mexico 87545

(Received 11 May 1992)

The quasiparticle energy spectra associated with some members of fullerene (curved graphitic geometries, e.g., C_{50}, C_{60}, C_{70}, and helical graphitic microtubules) are obtained analytically within the Hartree-Fock mean-field approximation. The magnetization and magnetic susceptibility are calculated in the presence of a strong external magnetic field at zero temperature. Interesting theoretical predictions such as the single quasiparticle excitation energies for C_{50}, C_{50}^+; C_{60}, C_{60}^+; C_{70} and C_{70}^+ as well as the presence of an extra peak in de Haas–van Alphen oscillations for a helical graphitic microtubule are discussed in terms of accessible experimental measurements.

Ever since the discovery[1] and mass synthesis[2] of fullerenes and coaxial helical graphitic microtubules[3] the focus has been to study a variety of their physical and chemical properties. One particularly interesting aspect is the effect of their curved geometry on the physical properties. Recent theoretical studies of magnetic ground states have already pointed to nontrivial topology of spin configuration on a C_{60} fullerene molecule[4] and the presence of "Landau fans" in the variation of quasiparticle spectrum with magnetic field for an electron gas on a sphere.[5] Here we intend to explore further consequences of a two-dimensional (2D) degenerate electron gas confined to curved geometries (fullerenes and helical graphitic microtubules). An additional motivation is to identify important physical attributes of these mesoscopic structures for potential applications in nanotechnology.

We have studied spherical fullerenes ranging from C_{32} to C_{98} but here we limit our discussion to C_{50}, C_{60}, and C_{70} for illustrative purposes. Within the Hartree-Fock (HF) formalism at zero temperature[6] we find that (i) at strong ($\geq$ 1 T) magnetic field all fullerenes except C_{32}, C_{50}, C_{72}, and C_{98} have a finite magnetic moment; (ii) all are diamagnetic (i.e., the slope of the magnetization vs magnetic field is negative); (iii) akin to a 2D (or 3D) electron gas the magnetization (and susceptibility) exhibit de Haas–van Alphen (dHvA) oscillations,[7] however, the oscillations occur at very high fields that are beyond the experimentally accessible range; (iv) the estimated value of the photoionization energy for C_{60} is in good agreement with the experimental measurement[8] and previous estimates,[9] and the single quasiparticle excitation energy for C_{60}^+ possibly explains the peak at ~7.8 eV observed in recent photoionization efficiency spectra.[8] In addition, we calculated photoionization energies for C_{50} and C_{70} and the single quasiparticle excitation energies for C_{50}^+ and C_{70}^+. For the smallest helical graphitic microtubule the dHvA oscillations (in magnetization, susceptibility) are found to exhibit an extra peak at ~169 T superimposed on the primary dHvA oscillation. All higher oscillations, which occur at extremely high values of magnetic field, have a twin-peak structure superimposed on them. We also briefly discuss results on a toroidal graphitic microtubule with the hope that they will be fabricated in the near future. Finally, we point to important potential technological applications of these carbon-based geometries, especially in the case of coaxial helical graphitic microtubules.

We consider a 2D degenerate electron gas on a spherical (C_{60}), a quasispherical (C_{50}, C_{70}) and a cylindrical (helical graphitic microtubule) surface. All spin-dependent interactions are neglected since they are negligible compared to the Coulomb interactions in the HF formalism.[6] We obtain analytically the following quasiparticle energy spectrum for closed-shell fullerenes at zero temperature:

$$\epsilon_l = \frac{l(l+1)\hbar^2}{2m_e a^2} - \frac{e^2}{a}\sum_{l',L}(-1)^{l'+L-l}\frac{2l'+1}{2L+1}(l'l00 \mid L0)^2, \tag{1}$$

where m_e denotes the mass of an electron, a is the radius of the fullerene, and $(l'l00|\ L0)$ are Clebsch-Gordan coefficients. The sum over l' is restricted to the highest occupied shell. In the above equation, closed-shell clusters can be found, e.g., l=3 corresponds to C_{32}, l=4 corresponds to C_{50}, l=5 corresponds to C_{72}, l=6 corresponds to C_{98}, and so on. Therefore, these closed-shell fullerenes have zero magnetic moment (within the shell model). Other C_n clusters correspond to partially filled shells. For instance, the C_{60} fullerene molecule has a partially filled l=5 shell (with 12 electrons removed). We assume that the mean field remains spherical for a partially filled shell; the quasiparticle energy spectrum of a partially filled cluster can then be obtained analytically.

When the magnetic field is applied the energy levels are split. The quasiparticle energy spectrum is calculated perturbatively:

 ©1992 The American Physical Society

$$\tilde{\epsilon}_{\ell m\sigma} \simeq \tilde{\epsilon}^{0}{}_{\ell m\sigma} + \frac{1}{12m_e}\left(\frac{eBa}{c}\right)^2 [1-(2\ell 0m|\ell m)(2\ell 00|\ell 0)] + \left(\frac{1}{12m_e}\right)^2\left(\frac{eBa}{c}\right)^4 \sum_{\substack{\ell' \\ \ell'\neq\ell}}^{\ell'_{\max}} \left(\frac{2\ell'+1}{2\ell+1}\right)\left[\frac{(2\ell' 0m|\ell m)^2(2\ell' 00|\ell 0)^2}{\epsilon_\ell - \epsilon_{\ell'}}\right], \quad (2)$$

where $\tilde{\epsilon^0}_{\ell m\sigma} = \epsilon_l + \frac{eB\hbar}{2m_e c}(m+\sigma)$ with ϵ_l given by Eq. (1), and $\sigma = \pm 1$. The magnitude of the second term is of the order of meV while the third term is of the order of μeV. Thus, the above results obtained by perturbation theory are quite accurate.

In Fig. 1 we show the discrete quasiparticle spectrum for C_{60}, C_{50}, and C_{70}. The energy gap between the highest (partially or fully) occupied level (l=5) and the first empty level (l=6) is 7.33, 8.58, and 8.0 eV, respectively. The gap for $C_{60}{}^+$, $C_{50}{}^+$, and $C_{70}{}^+$ is 7.07, 8.23, and 7.74 eV, respectively. Note that a closed-shell cluster is the most stable; so the energy gap for C_{50} is the largest, and C_{70} is the next largest in magnitude. The experimental photoionization efficiency spectra[8] show a peak for $C_{60}{}^+$ at about 7.8 eV; it is possibly the single particle excitation energy 7.07 eV we calculated. The ionization potential consists of two terms. The first can be found by using the Koopmans theorem,[10] i.e., the negative of the highest quasiparticle energy level. This is the energy required for an electron to be free on the surface. The second term is the energy cost of removing the free electron from the surface to infinity; it is estimated electronically to be equal to e^2/a, with a being the C_{60} fullerence molecule radius. This estimate gives us the ionization potentials for C_{60}, C_{50}, and C_{70} to be 8.86, 13.57, and 12.37 eV, respectively. Comparing with the experimental estimation[8] of the ionization potential 7.54±0.04 eV (and previous estimates[9]) for C_{60}, our result is in good agreement with the data within 10%. For a closed-shell cluster, the ionization potential must be larger due to the stability of the cluster. Our results reflect this fact. We have used for C_{60}, C_{50}, and C_{70}, radii of 3.45, 3.3, and 3.65 Å, respectively. The bandwidths of C_{60}, C_{50}, and C_{70} are predicted to be 18.0, 12.35, and 15.04 eV, respectively, in reasonable agreement with the tight-binding[11] and local-density-approximation[12] (LDA) calculations for C_{60}.

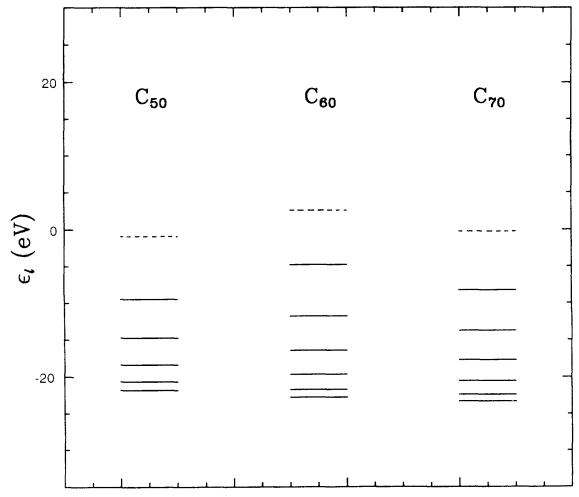

FIG. 1. Quasiparticle energy spectrum for C_{50}, C_{60}, and C_{70} in the absence of a magnetic field. The dashed lines denote the lowest unoccupied energy levels.

The quasiparticle energy spectrum for a helical graphitic microtuble[3] in an external magnetic field applied along the tube axis can be calculated exactly, and is given by

$$\epsilon_{n,q}(\lambda) = \frac{\hbar^2}{2m_e a^2}[q^2+(n+\lambda)^2] - \frac{e^2}{\pi a}\sum_{p=-N_l}^{N_u}\int_{q_1}^{q_2} dx\, K_{n-p}(|x|)\, I_{n-p}(|x|), \quad (3)$$

where

$$q_1 = q - \sqrt{\ell_f^2-(p+\lambda)^2},$$
$$q_2 = q + \sqrt{\ell_f^2-(p+\lambda)^2},$$

with N_u and N_l the highest and lowest occupied subband indices, and $l_f^2 = 2m_e a^2\epsilon_f/\hbar^2$ the normalized Fermi wave vector. Also, in the above a denotes the radius of the helical graphitic microtubule and K and I are modified Bessel functions. We have defined all wave vectors in units of the microtubule radius a, and λ=Φ/Φ_0 with Φ=$\pi a^2 B$ and the unit of flux Φ_0=$(2\pi\hbar c/e)$. Note that the spectrum is continuous along the microtubule direction but quantized along the angular direction. If, on the other hand, we choose a finite length (L) helical graphitic microtubule with periodic boundary conditions we obtain a toroidal graphitic microtubule with a completely quantized spectrum given by the above equation except that now the wave vector q is quantized as $q = (2\pi la/L)$.

The Fermi energy and the subband filling indices (N_u and N_l) are calculated at fixed surface electron density. The surface electron density is approximated by $\sigma = 4/(\pi r)^2 = 63.14\ \mathrm{nm}^{-2}$, in a circle of radius $r/2$ on the graphite surface, where $r = 1.42$ Å is the C-C bond length. Thus, we solve

$$\sigma = \frac{\sigma_0}{2}\sum_{p=-N_l}^{N_u}\sqrt{l_f^2-(p+\lambda)^2} \quad (4)$$

for l_f^2, N_l, and N_u. The quantity σ_0 is defined as $\sigma_0 = 2/(\pi a)^2$ and depends on the microtubule radius a. The solution of the above equation gives the Fermi energy.

In Fig. 2 we show the quasiparticle energy subband spectrum for a helical graphitic microtubule as a function of the wave vector (along the microtubule axial direction). The spectrum is discrete in the angular direc-

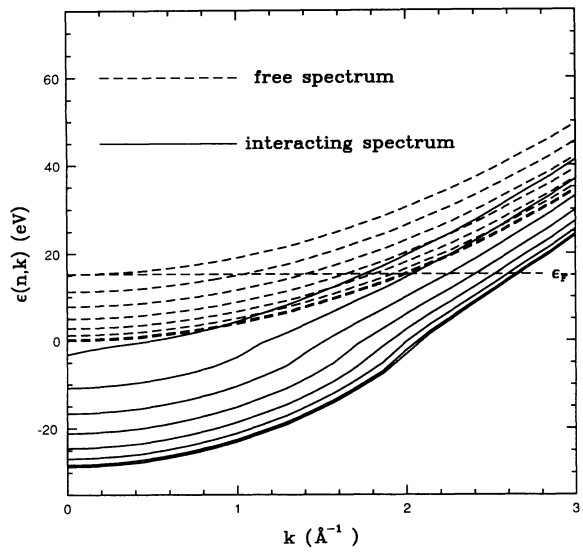

FIG. 2. Quasiparticle energy spectrum for a helical graphitic microtubule (a=0.35 nm) as a function of the wave vector in the absence of a magnetic field. ϵ_F is calculated from the free-particle energy spectrum.

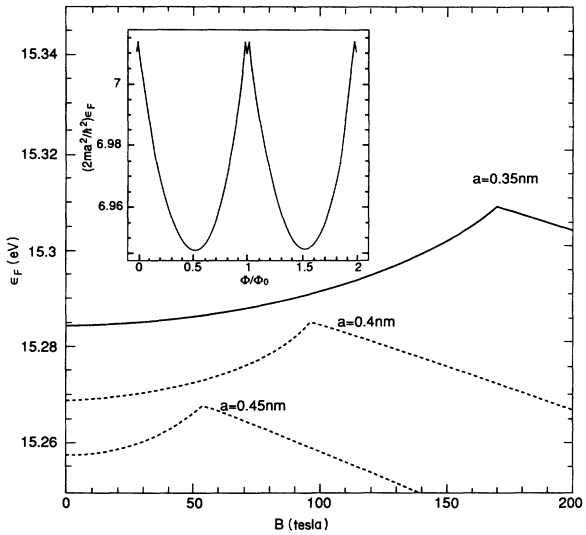

FIG. 3. Fermi energy ϵ_F as a function of the applied magnetic field associated with a helical graphitic microtubule for three different radii. The inset shows the twin-peak structure at very high magnetic fields for the smallest helical graphitic microtubule (a=0.35 nm).

tion due to the finite microtubule geometry. Note that the free-particle energy subbands are parabolic (dashed curves) but shift down in energy (symmetric about the vertical axis) after the inclusion of the interaction (Fock) term (solid curves). The calculated bandwidth (at q=0) is 15.2 eV, which is comparable to 14.4 eV predicted by LDA.[13] Furthermore, by suitably adjusting the curvature (the radius a) of the microtubule, one can control the quasiparticle level spacing and adjust the strength of the Coulomb interaction. At a given value of q one can also deduce the optical excitation energy of a helical graphitic microtubule from Fig. 2.

The Fermi energy obtained from the tree-particle energy spectrum is plotted as a function of the magnetic field in Fig. 3 for helical graphitic microtubules of three different radii. With increasing magnetic field, the separation between subbands increases. The cusp in the Fermi energy results from a subband crossing the Fermi surface. This kind of level crossing gives rise to two different types of oscillations. First, the primary dHvA oscillations which occur at very large field values (i.e., Φ/Φ_0 an integer, see the inset) and result from subband reordering. Second, there is a single peak (for $\lambda \cong 0$) superimposed on the primary dHvA oscillation due to the broken degeneracy that results from the Zeeman splitting of the subbands. At very large fields there is a twin-peak structure superimposed on all higher primary dHvA oscillations due to the double degeneracy of each subband (see the inset). The splitting of a twin peak is a direct measure of the subband splitting of $n = 1, 2, 3, \ldots$ levels.

The smallest helical graphitic microtubule has a radius equal to that of a C_{60} fullerene molecule, i.e., 3.5 Å. The first peak in this case occurs at ~169 T. As the helical graphitic microtubule radius is increased the peak position shifts to lower field values. However, the peak height also decreases proportionally. As observed by Iijima,[3] a helical graphitic microtubule can contain from 2 to 50 coaxial microtubules varying in radius from 2 to 15 nm and up to 1 μm in length. Therefore, experimentally for a pure sample one would expect the number of peaks, and their location and magnitude, to be directly related to the number of microtubules in a coaxial helical graphitic microtubule and their radii.

We calculated the magnetization [at zero temperature and strong magnetic field ($\geq$ 1 T)] by finding the derivative of the free energy with respect to the magnetic field. We do not give the analytic expression for M here since the derivation is straightforward, nor do we plot M as a function of B. However, we find that C_{50} has no magnetization whereas C_{60} and C_{70} saturate at $M = 31$ and 11 in the units of the Bohr magneton, respectively. Also, we note that the value of M is the same for fullerenes which have the same number of either electrons or holes on the highest partially filled shell. Thus, for example, C_{60} (l=5 with 12 holes) and C_{62} (l=5 with 12 electrons) have the same $M = 31$. The slope of all magnetization curves is found to be negative indicating that all spherical fullerenes are *diamagnetic*. The dHvA oscillations occur at extremely large fields.

We also calculated the magnetization of a helical graphitic microtubule as a function of the applied magnetic field; however we do not plot it here. The magnetization increases extremely slowly, and linearly with the field. At around 169 T (for a helical graphitic microtubule with radius 3.5 Å) a sharp spike is predicted which should be observable experimentally. For a coaxial geometry (assuming negligible interaction between the adjacent microtubules) one would expect a series of spikes below 169 T. The number of spikes would correspond to the number of microtubules in the coaxial structure. At very large values of the field there are twin spikes superimposed on the dHvA oscillations (cf. Fig. 3).

The derivative of magnetization with respect to the applied magnetic field gives magnetic susceptibility of the system. For spherical fullerenes the value of χ is consistent with previous investigations.[14] At magnetic fields below the value of the first dHvA oscillation the χ for C_{60}, C_{50}, and C_{70} is 0.003 63, 0.002 76, and 0.004 56 in the units of Bohr magneton/T, respectively. Note that the value increases with increasing number of carbon atoms in a fullerene. In Fig. 4 we depict the variation of χ with magnetic field for helical graphitic microtubules of three different radii. For the smallest helical graphitic microtubule (a = 3.5 Å) the χ is almost zero except around 169 T where a sharp peak is predicted. For a coaxial structure many such peaks are expected below 169 T. We have not shown the twin peaks at extremely high fields that are superimposed on the dHvA oscillations. The magnitude of these peaks can be measured experimentally and provides information about the underlying subband structure of the helical graphitic microtubules in a magnetic field.

In summary, we have calculated the quasiparticle energy spectra for C_{60}, C_{50}, and C_{70} as well as for their ionized clusters. The single quasiparticle excitation energies are predicted and the ionization potentials are estimated. The results are consistent with the recent available experimental data. We also presented results at zero temperature for the magnetic response of various spherical fullerenes and coaxial helical graphitic microtubules. Finite-temperature results and thermal properties will be reported elsewhere. The role of finite curved geometry is clearly manifested in the finite magnetization (at fields $\geq$ 1 T) and diamagnetic response of some of the fullerenes, and in the M and χ peak structures of coaxial helical graphitic microtubules below 170 T (as contrasted with a planar 2D electron gas). The spherical fullerenes are found to be diamagnetic with different slopes (as compared to a 2D planar electron gas). For the helical graphitic microtubules we have shown evidence of the presence of an extra peak superimposed on the first dHvA oscillation which should be accessible with special (explosive) dHvA experiments.[15] Furthermore, for coaxial helical graphitic microtubules the number of peaks superimposed on the first dHvA oscillation directly indicates the number of microtubules in the coaxial structure and their radii (assuming the 2D electron gas on each individual microtubule is not interacting with its neighboring microtubules). We believe it is possible to synthesize a single (or a coaxial) toroidal graphitic microtubule provided that the radius of the torus is large enough to accomodate the strain generated by folding a tube into a torus.

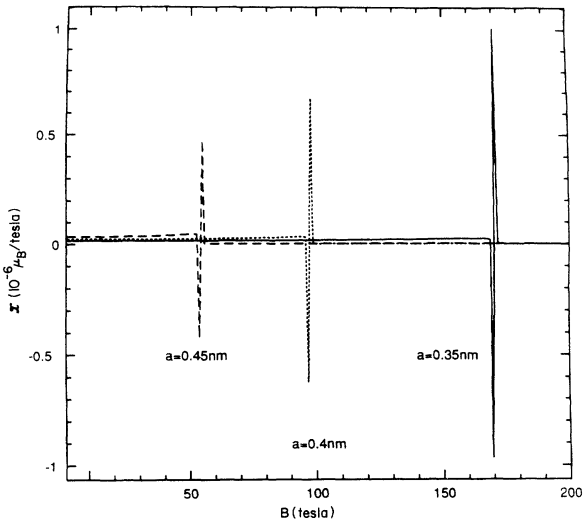

FIG. 4. Magnetic susceptibility as a function of the applied magnetic field associated with a helical graphitic microtubule for three different radii.

We have also studied the plasmon excitations for various fullerenes and multichannel transverse-electric (TE) mode propagation in the coaxial helical graphitic microtubules. These results along with their implications for helical graphitic microtubules as waveguides will be reported elsewhere.[16]

We acknowlegde fruitful discussions with J. Zhang, F. Zeng, A.F. Voter, S.A. Trugman, R.L. Martin, and F.M. Mueller. This work was supported by the U.S. DOE.

[1]H.W. Kroto, J.R. Heath, J.R. O'Brien, S.C. Curl, and R.E. Smalley, Nature **318**, 162 (1985).
[2]W. Krätschmer, L.D. Lamb, K. Fostiropoulos, and D.R. Huffman, Nature **347**, 354 (1990).
[3]S. Iijima, Nature **354**, 56 (1991).
[4]D. Coffey and S.A. Trugman, Phys. Rev. Lett. **69**, 176 (1992).
[5]J.H. Kim, I.D. Vagner, and B. Sundaram, Phys. Rev. B (to be published).
[6]See, e.g., A.L. Fetter and J.D. Walecka, *Quantum Theory of Many-Particle Systems* (McGraw-Hill, New York, 1971), p. 121.
[7]A.V. Gold, in *Solid State Physics*, edited by J.F. Cochran and R.R. Haering (Gordon and Breach, New York, 1968).
[8]I.V. Hertel *et al.*, Phys. Rev. Lett. **68**, 784 (1992).
[9]D.L. Lichtenberger *et al.*, Chem. Phys. Lett. **176**, 203 (1991), and references therein.
[10]See, e.g., C. Kittel, *Quantum Theory of Solids* (Wiley, New York, 1963), p. 83.
[11]G.F. Bertsch, A. Bulgac, D. Tománek, and Y. Wang, Phys. Rev. Lett. **67**, 2690 (1991).
[12]S. Saito and A. Oshiyama, Phys. Rev. Lett. **66**, 2637 (1991).
[13]J.W. Mintmire, B.I. Dunlap, and C.T. White, Phys. Rev. Lett. **68**, 631 (1992).
[14]V. Elser and R.C. Haddon, Nature **325**, 792 (1987); Phys. Rev. B **36**, 4579 (1987); R.C. Haddon *et al.*, Nature **350**, 46 (1991); R.S. Ruoff *et al.*, J. Phys. Chem. **95**, 3457 (1991); J.D. Thompson *et al.* (unpublished).
[15]See, e.g., C. M. Fowler *et al.*, Phys. Rev. Lett. **68**, 534 (1992).
[16]P.S. Davids, L. Wang, A. Saxena, and A.R. Bishop (unpublished).